



## A novel weld seam detection method for space weld seam of narrow butt joint in laser welding

Wen Jun Shao, Yu Huang, Yong Zhang\*

State Key Lab of Digital Manufacturing Equipment and Technology, School of Mechanical Science and Engineering, Huazhong University of Science and Technology, Wuhan, China

### ARTICLE INFO

#### Article history:

Received 12 May 2017

Received in revised form 1 September 2017

Accepted 20 September 2017

Available online 7 October 2017

#### Keywords:

Structure light

Vision sensor

Seam detection

Butt joint

Laser welding

### ABSTRACT

Structured light measurement is widely used for weld seam detection owing to its high measurement precision and robust. However, there is nearly no geometrical deformation of the stripe projected onto weld face, whose seam width is less than 0.1 mm and without misalignment. So, it's very difficult to ensure an exact retrieval of the seam feature. This issue is raised as laser welding for butt joint of thin metal plate is widely applied. Moreover, measurement for the seam width, seam center and the normal vector of the weld face at the same time during welding process is of great importance to the welding quality but rarely reported. Consequently, a seam measurement method based on vision sensor for space weld seam of narrow butt joint is proposed in this article. Three laser stripes with different wave length are project on the weldment, in which two red laser stripes are designed and used to measure the three dimensional profile of the weld face by the principle of optical triangulation, and the third green laser stripe is used as light source to measure the edge and the centerline of the seam by the principle of passive vision sensor. The corresponding image process algorithm is proposed to extract the centerline of the red laser stripes as well as the seam feature. All these three laser stripes are captured and processed in a single image so that the three dimensional position of the space weld seam can be obtained simultaneously. Finally, the result of experiment reveals that the proposed method can meet the precision demand of space narrow butt joint.

© 2017 Elsevier Ltd. All rights reserved.

### 1. Introduction

Laser welding is a very promising welding method in terms of high energy density, narrow HAZ, low shape distortion of components, and high welding speed, which is one of the most important implementation of laser technology. As a result of the development of high power lasers as well as the improvement of the optical fiber transmission technology for laser beam, recent years have seen a tremendous growing of laser welding in automotive industry, shipping industry, and aircraft industry.

It is difficult for traditional welding method to weld materials with high hardness, high melting point, or high brittleness. On the contrary, laser welding has the characteristics of non-contact, deep penetration, high precision, flexible, and compatible with complex shapes of all sizes that it is especially suitable for materials such as TC4 in aircraft industry. As a result, the increase of laser welding for rocket motor nozzle, skin structure and inlet structure in aircraft industrial is especially noticeable. However, as

compared to traditional welding methods, laser welding demands stricter assembly quality. Moreover, aircraft industry gives top priority to the weight that many of its structures are made of titanium alloy sheet with thickness less than 2 mm. That means the seam of the butt joint is very narrow and without misalignment that the seam feature is difficult to be extracted by an ordinary vision sensor based on optical triangular principle.

As for butt joint formed by metal sheets with thickness of 0.2 mm, both gap and misalignment of its seam should be less than 0.1 mm at the assembling stage [1]. To ensure welding quality, the laser beam focus should follow the seam center exactly and there should be appropriate defocus amount during laser welding process. At the same time, welding speed and welding power should be adjusted according to the seam width. Especially, as the diameter of the laser beam focus is about 0.3 mm, the offset between the laser focus center and the weld seam center should be less than 0.1 mm. Otherwise, it may cause asymmetric heat source along the weld seam center line, which may result in poor welding quality or even welding failure. Meanwhile, to obtain a better welding quality, there should be appropriate angle between the laser optical axis and the normal vector of the weld face [2–4]. In a word, the weld seam center, seam width and the normal vector

\* Corresponding author.

E-mail address: [zhangyong904@163.com](mailto:zhangyong904@163.com) (Y. Zhang).

of its local weld face should be precisely measured before we can get satisfactory welding result.

Generally, there are apparent imaging features in the weld joint when laser structure light is projected on weld face. In addition, much of the noise light caused by welding could be eliminated by optical filter, which makes this measurement very precise and robust. This is the reason that laser structure light has been widely used in seam measurement for laser welding [5]. In literature, there are numerous researches on weld seam measurement by using structure light. Among them, the detection of the butt joint with V-shaped groove or T-shaped groove by structure light are very success because the projected structure light get bended in the weld joint. The bended structure light forms very apparent imaging features, which can be easily detected, makes the vision measurement very effective.

As for V-groove butt joint, a new image process algorithm consisting of particle filtering and self-adapting dynamic window was proposed by Tao et al. for this kind of joint, which was very robust in very hostile welding environments [6]. Wu et al. introduced a modified Hough algorithm for image process in weld seam tracking for V-groove butt joint [7]. He et al. proposed a seam extraction algorithm based on orientation saliency for V-groove butt joint [8]. Prasarn Kiddee et al. used cross mark structured light to detect V-groove butt joint [9]. A modified template matching method was used to detect the edges of V-shaped groove, which greatly reduced computational cost in image process.

As for T-shape weld joint, Huang et al. used structure light based vision sensor to detect weld seam in a dual laser welding system for T-joint in aircraft industry [10].

Not only that, laser structure light based measurement was very suitable for butt joint, whose gap is larger than 0.1 mm. Zhang et al. reported a novel laser vision sensor based on structure light for weld seam detection on wall-climbing robot, which can capture 3D information of the weldment with very low measurement error [11].

However, some noteworthy researches [14,15] indicated that laser structure light was ineffective for narrow butt joint, especially those whose gap is smaller than 0.1 mm.

In order to tackle this problem, passive light vision technology was adopted instead of structure light based vision sensor, in which images were captured by using arc light or auxiliary light source. Xu et al. tried to solve the seam tracking problem for butt joint arc welding of metal sheet by using passive vision system [12]. To avoid processing images with too much noise, an image selecting method was investigated. The seam position precision range was controlled to be within  $\pm 0.3$  mm, which was obtained by an improved Canny edge detection algorithm. Fang et al. developed a visual seam tracking system for butt weld of thin plate [13]. The seam was too narrow to be detected by the structure light that the seam position in horizontal direction was extracted from images captured on natural lighting. The Structure light was only used to detect the seam position in vertical position. The seam tracking accuracy of the system in horizontal and vertical directions were 0.2 mm and 0.1 mm, respectively. Due to the same reason, Chen et al. did not use structure light to detect narrow seam [14]. Instead, they presented a vision sensor system consisting of a CCD camera and a white light-emitting diode (LED) light source, which is mainly used to detect narrow seam whose width is generally less than 0.2 mm. Since there were sparks and fuming during welding process, the captured images in this way contained too much noise. So, a set of feature extraction algorithms, such as profile extraction, Hough transform, and least-square fitting, were employed to extract weld seam. Gao et al. aimed at detecting narrow butt weld by using a magneto-optical sensor [15]. It was also argued that this kind of weld joint was too narrow to measure by

structure light. However, his method was only applicable to magnetic materials.

Most recently, Wang et al. developed a set of seam measurement system, which used multiple optical magnifier to detect narrow weld seam [16]. Measurement accuracy for the seam width and seam position were 6  $\mu\text{m}$  and 8  $\mu\text{m}$ , respectively. But, the field of view was 1.3  $\text{mm}^2$ , which made its application very limited. Particularly, weld seam detecting sensors produced by companies, such as Meta Vision Systems Ltd, were widely used in industry field. Nonetheless, as for butt joint, these vision sensors were ineffective when seam gap was less than 0.1 mm.

On the one hand, vision system based on passive light sensor can obtain more seam feature, which is beneficial for the measurement of narrow butt joint. On the other hand, it's very sensitive to light noise during welding process. On the contrary, vision system based on active light sensor can eliminate much of the light noise by adopting optical filter and it's more suitable for three-dimensional measurement such as normal vector measurement of the weld face. But, as the weld gap is less than 0.1 mm, the projected structure light deforms slightly around the joint that it is hard to extract the seam position.

Therefore, a novel seam measurement system, which effectively combines the superiority of passive light sensor and active light sensor, is designed in this article. Three laser stripes are used to detect the weld seam in this measurement system. Two of them are for three-dimensional measurement purpose, which are used to get normal vector of local weld face by measuring the profile of the weld face; one of them is used for two-dimensional measurement purpose, which is used as light source to extract weld seam edge.

It's well known that optical triangulation method based on structure light is very applicable for three-dimensional measurement. In addition, it's very feasible to extract weld seam edge according to difference in gray value by two-dimensional image measurement. Applying structure light based three-dimensional measurement or two-dimensional image measurement for weld seam detection is not new idea and not the focus of this article. Instead, the contribution of this article is the combination of the two methods, in which the proposed vision sensor can detect narrow butt joint with seam gap less than 0.1 mm. The contribution of our system lies in the following two aspects:

1. It provides an effective vision sensor to measure butt joint with no misalignment and width less than 0.1 mm by combining traditional methods.
2. Weld seam width, seam center and normal vector can be obtained in a single image by one measurement.

As the popularization of laser welding technology, and the harsh assembling precision requirements and strict weld torch position control demands, the demand for high precision weld seam detection technology grows daily. The proposed method is not only applicable for butt joint in aircraft industrial but also can meet butt joint detection requirements in other industrial applications.

## 2. Experiment setup

### 2.1. Task analysis

The seam measurement principle of traditional optical triangulation by structure light is shown in Fig. 1. The shape, position and gray value of the laser stripe would be changed when projected on the groove or gap of the weld face. Then, the seam width and seam

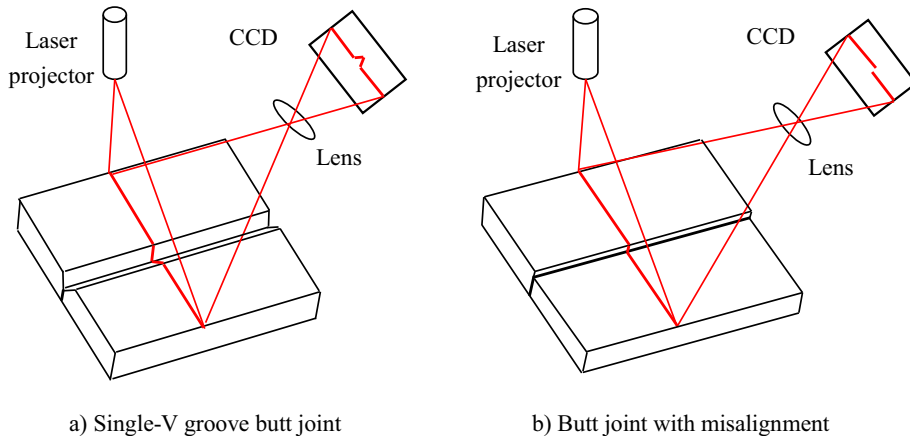


**Fig. 1.** Seam measurement by optical triangulation with structure light.

center can be obtained by image process according to the corresponding change in the seam image. As shown in Fig. 1, the laser stripe gets distorted much by V-groove butt joint or butt joint with considerable misalignment, which reduces the difficult of seam feature extraction. Consequently, the measurement of seam width and seam position is very precise and steady.

However, as the comparison shown in Fig. 2, the deformation of the laser stripe is too tiny to be detected when the gap width of the butt joint is less than 0.05 mm and without misalignment. Therefore, as for weld seam of this type, it's very difficult to obtain the seam width and seam position precisely and steadily by the laser stripes.

As shown in Fig. 3, butt joint formed by two thin metal plates is very typical and common weld joint type. To ensure high welding quality, not only should the laser focus follow the seam center precisely but also the defocus amount and the incident angle should be controlled accurately. Thus, the vision sensor for weld seam

proposed in this article should have the ability to measure seam width, seam center and the normal vector of the weld face. Particularly, the prerequisite is that it can overcome the disadvantages of the optical triangulation method based on laser stripes.

## 2.2. Design of the vision sensor

As shown in Fig. 4, the proposed vision sensor consists of one CCD camera, one telecentric lens, four laser stripe projectors, and one optical filter. Their parameters are shown in Table 1. In order to measure narrow weld seam with a minimum width of 0.01 mm, the vision sensor should have 0.01 mm resolution at least. CCD camera with pixel size of 7.4  $\mu\text{m}$  and telecentric lens with 1.0 times magnification is chose so that the proposed vision sensor has resolution of 7.4  $\mu\text{m}$ . Telecentric lens is adopted because its image magnification is independent of the object's distance or position in the field of view. Moreover, telecentric lens has lower

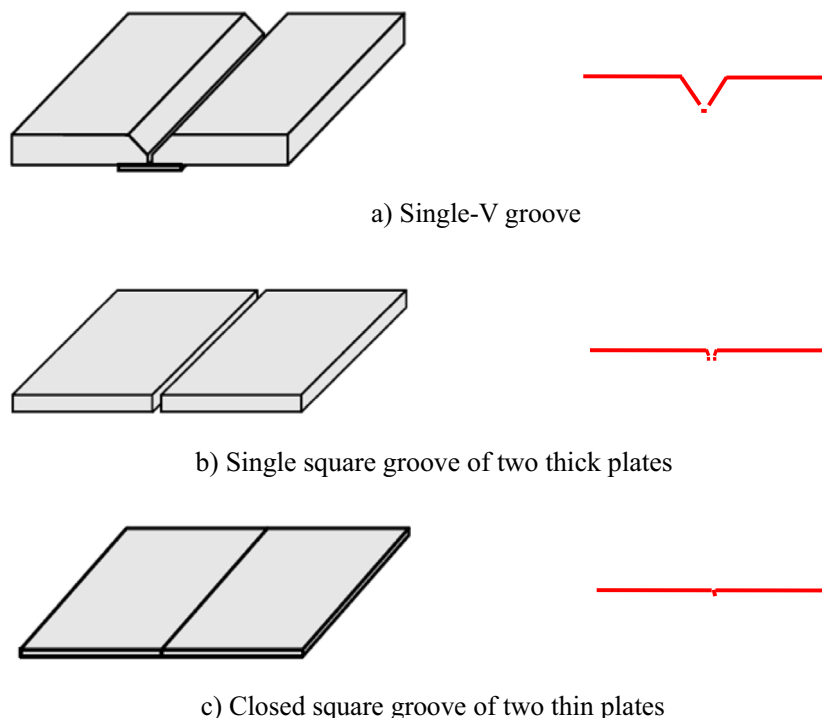


**Fig. 2.** Comparison of deformation amount under different weld joint.

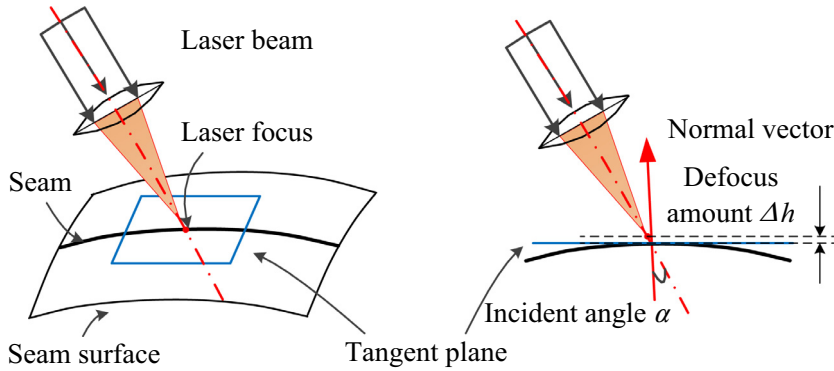


**Fig. 3.** Adjustment of focus center, defocus amount and incident angle during welding.

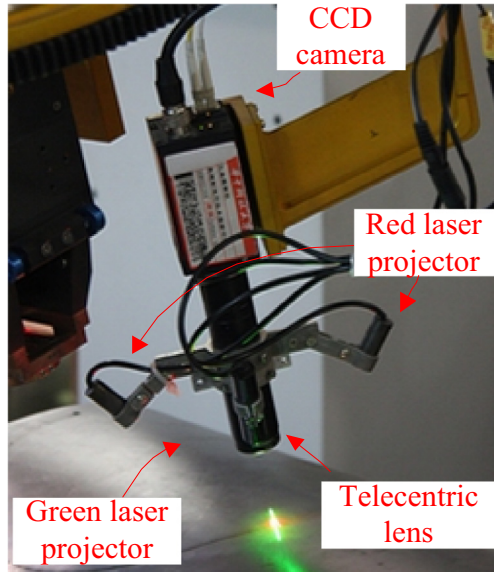


**Fig. 4.** The structure of the weld seam sensor.

lens distortion, which is very crucial for high precise measurement. As the aperture of telecentric lens is narrow, only highly collimated rays are admitted, resulting much of the noise light is eliminated. The most frequently used CCD cameras have better imaging characteristic when light source of middle or short wavelength is adopted. So, red laser stripe projector with 650 nm wavelength is adopted in order to obtain structure light images with high quality. On the contrary, light source with short wavelength can make the narrow seam feature more distinctive. Hence, green laser stripe projector with 532 nm wavelength is adopted in order to obtain seam feature with high definition. In order to selectively transmit light in a particular range of wavelengths, specially customized optical filter is used. The optical filter is made to have two peaks rather than a single band, which can pass wavelengths near 532 nm and 650 nm and have cutoff wavelengths in 700–1064 nm and 200–450 nm.

**Table 1**  
Parameters of weld seam vision sensor.

Item	Parameters
CCD camera	Pixel size: 7.4 μm × 7.4 μm; image area: 1000 × 1000; frame rate: 60 f/s
Telecentric lens	Magnification time: 1.0; telecentric range: 5 mm; depth of field: ±1.25 mm
Stripe projectors	Diameter of field of view: 11 mm; image-side aperture: 0.02;
Optical filter	Wavelengths of red laser stripe: 650 nm; Wavelengths of green laser stripe: 532 nm Bandpass: 480–690 nm; two peaks near 532 nm and 650 nm

### 2.3. The principle of weld seam measurement based on three-laser-tripe vision sensor

#### 2.3.1. The measurement of normal vector

As shown in Fig. 5, there are different intersection angles between the two red structure light planes and the optical axis of CCD camera so that the CCD camera and the two red laser projectors can form a three-dimensional measurement system for seam normal vector measurement. Accordingly, as shown in Fig. 6(a), there are two narrow laser stripes in the captured seam image when the two red structure light project on weld face. According to optical triangular measurement, the three-dimensional position of weldment profile can be calculated when the center points of laser stripes are obtained by image process. Because the camera's field of view is small, the local weld face can be regarded as a plane. Therefore, the approximate plane

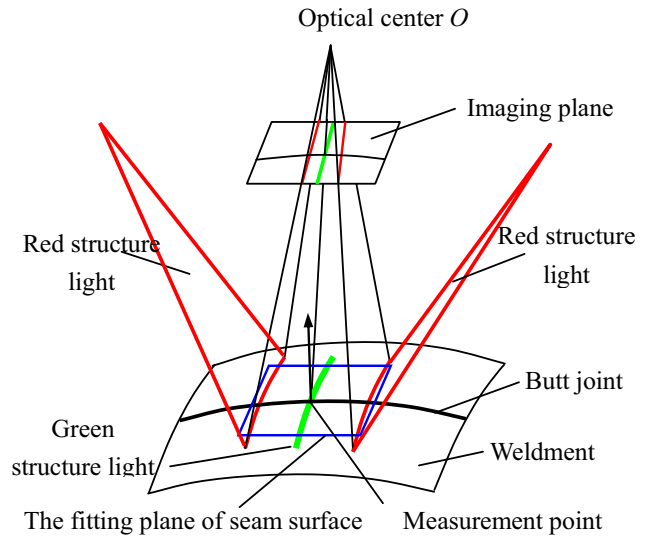


**Fig. 5.** Measurement principle of the proposed weld seam sensor.

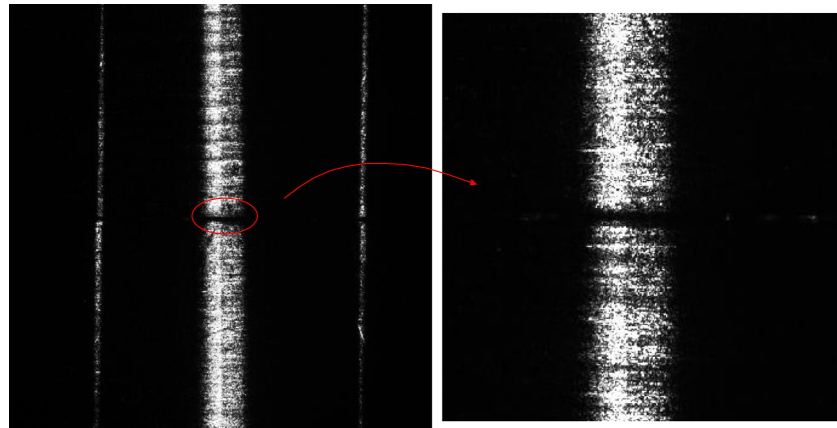


**Fig. 6.** Weld seam image captured by the proposed vision sensor.

equation of the local weld face can be calculated by carrying least square fitting method to the obtained three-dimensional points of the weldment profile. Finally, the normal vector of the local weld face is calculated according to the plane equation.

### 2.3.2. The measurement of seam center and width

As shown in Fig. 5, the two green structure light projectors and the CCD camera form a two-dimensional measurement system for seam center and width measurement. As shown in Fig. 6, the two green structure light planes are overlapped to form one bold stripe such that the seam feature is more distinctive. The position of the optical axis of the camera is designed to pass through the two structure-light planes, which makes the green laser stripe always in the center of the image and its shape doesn't change with the weld face. That means the seam feature can be extracted in a fixed area in the image center. As shown in Fig. 6, the gray value of weld seam gap is lower than that of the weld face. Accordingly, the edge and the center of the seam gap can be extracted by image process. After that, the image coordinates of the points in seam edge and seam center can be projected to the fitted plane according to pin-hole imaging principle so that the three dimensional coordinates of the points in seam edge and seam center can be obtained.

## 3. Image process

According to the described measurement principle, center points extraction of the two red laser stripes and edge detection of weld seam in the green laser stripe are the purposes of image process. Due to the different feature extraction purposes and the different characteristics of these two kinds of laser stripe, the corresponding image process method is different. Image process flow charts for these two kinds of laser stripe are shown in Figs. 7 and 8.

### 3.1. Center points extraction of the two red laser stripes

Let  $P = \{(i,j) | 1 \leq i \leq 1000; 1 \leq j \leq 1000\}$  represents the weld seam, where the image size is  $1000 \times 1000$ . According to waveforms of the gray value in Fig. 9, the width of each red laser stripe is about 25 pixels. In order to improve the image process speed, the region of interest which is denoted by  $ROI_r$  should be extracted. As the flow chart shown in Fig. 7, the rough center points of the red stripes are firstly located. A search window with 25 pixels width and 1 pixel height is used to find the rough center points of the two red laser stripes. Let  $S$  denote the search window and let  $S_{ij}$  be the translation of  $S$  so that its origin is located at  $(i,j) \in P$ . The green laser stripe is always in the center of the image, which is

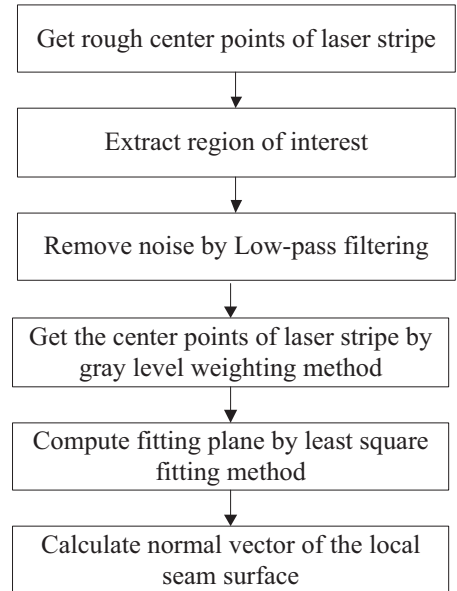


**Fig. 7.** Image process for red laser stripes.

determined by the design of the proposed vision sensor. By taking advantage of this characteristic, there is no need to search in the center of the image, which reduces the search time. To ensure fast image process, the search window moves and searches in the manner depicted in Fig. 10. In this way, after the search window located the rough center point by searching through the first row, the search windows only need to search around the previously located rough center point in next row. When the value of Eq. (1) in each row reaches maximum, the center point in search window is regarded as the rough center point of the laser stripe. As shown in Fig. 11, after all of the rough center points are obtained, the region of interest  $ROI_r$  is determined. It can be found that each row in the region of interest is centering at rough center point and has the width of 25 pixels.

$$Sum(S) = \sum_{(s,t) \in S} P(s,t) \quad (1)$$

As shown in Fig. 12, a low-pass filter is used to remove noise in  $ROI_r$ . Let  $B_{ij}$  denote a window or a flat structuring element, which is used to scan every row in  $ROI_r$ . The size of  $B_{ij}$  is  $1 \times 5$ . The equation of the low-pass filter is given as follows.

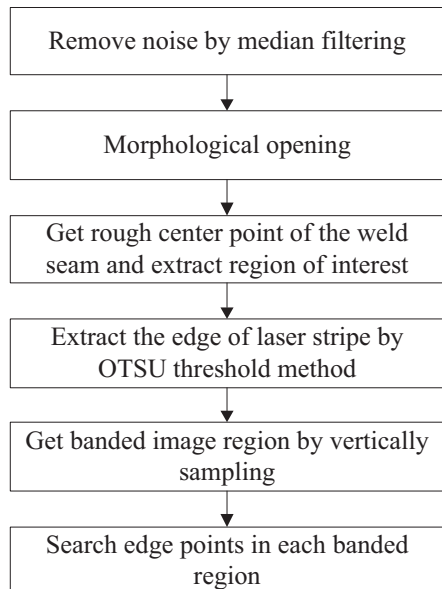


**Fig. 8.** Image process for green laser stripe.

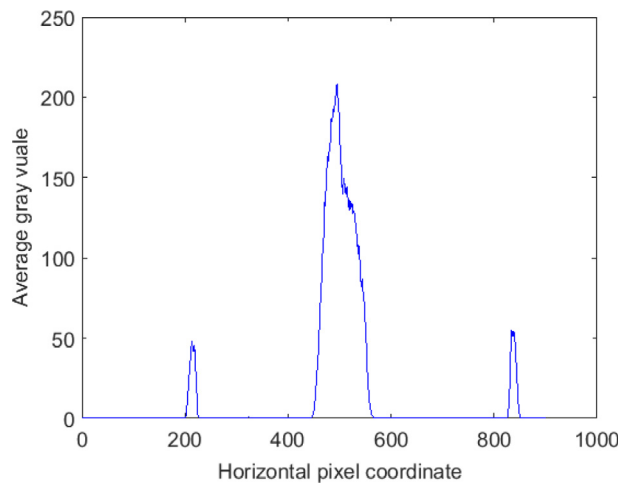


**Fig. 9.** Waveforms of the gray value.

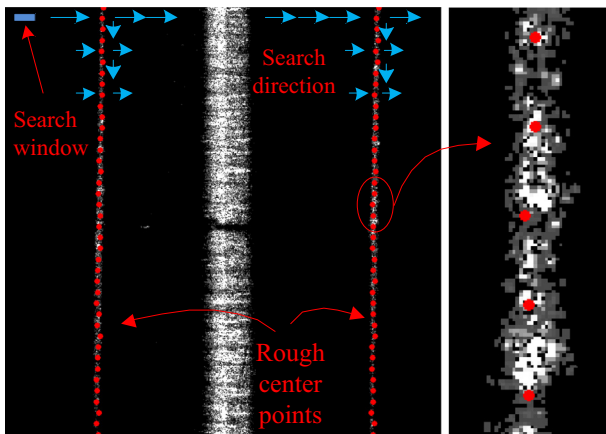


**Fig. 10.** Rough center point.

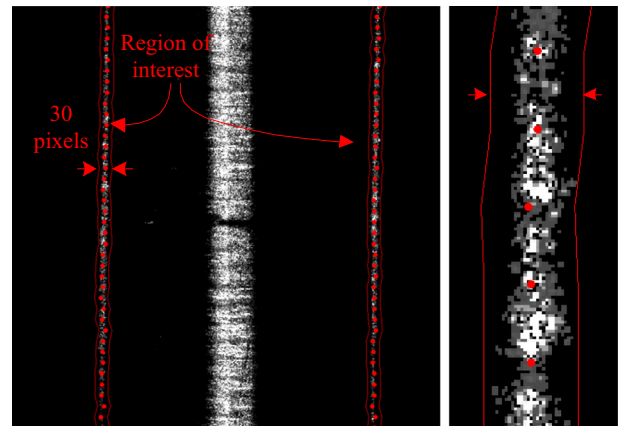


**Fig. 11.** The extraction of region of interest.

$$\begin{aligned} ROI_{rm}(i,j) = & k_0 \times ROI_r(i,j-2) + k_1 \times (ROI_r(i,j-1) + ROI_r(i,j+1)) \\ & + k_2 \times (ROI_r(i,j) + ROI_r(i,j+2)) \end{aligned} \quad (2)$$

The value of the coefficients of the low-pass filter are  $k_0 = 0.39124$ ,  $k_1 = 0.26453$  and  $k_2 = 0.0797$ .  $ROI_{rm}(i,j)$  is the gray value in row  $i$  and line  $j$  of the  $ROI_r$  after the low-pass filter process.

As shown in Fig. 13, gray level weighting method is used to get center points with higher accuracy. The center position  $C_i$  in every row is computed as follows,

$$C_i = i * \sum_j ROI_{rm}(i,j) / \sum_j ROI_{rm}(i,j) \quad (3)$$

Then, these center points in image coordinate are transformed to the machine coordinate. After all the center points in the two red laser stripes are obtained, least square fitting method is carried out to compute the fitting plane. The fitting plane is regarded as the approximate plane of the local weld face. Consequently, the normal vector of the fitting plane and the distance between the laser focus and the fitting plane can be computed, which are used to control the incident angle and defocus amount of the welding torch.

### 3.2. Edge detection of weld seam in the green laser stripe

The flow chart of edge detection algorithm of the weld seam in green laser stripe is shown in Fig. 8. Similarly, it can be found out in Fig. 9 that the width of the green laser stripe is about 100 pixels. Due to the design of the proposed vision sensor, the green laser stripe is always in the center of the image. By taking this advantage, only part of the weld seam image should be processed. As shown in Fig. 14, let  $I$  denote this area, which has the width of 100 pixels and its centerline is overlap with the centerline of the whole image. So, only very small fixed area of the image has to be processed, which leads to dramatically reduction in computation time.

Firstly, as shown in Fig. 15, median filter is used to remove noise. The size of the structuring element is  $3 \times 3$ , which is used to scan every pixel in  $I$ . Let  $I_f(i,j)$  denote the gray value in row  $i$  and line  $j$  of the  $I$  after the median filter process.

Secondly, as shown in Fig. 16, morphological opening method is adopted to remove bright pixels from the background (weld face), which can further reduce the noise and make the seam feature more apparent. Let  $B_{ij}$  denote a window or a flat structuring element whose size is  $5 \times 5$ . Then, the erosion  $\varepsilon_B(I_f)$  of an image  $I_f$  by structuring element  $B_{ij}$  is used to constructing a morphological filter, which is given as

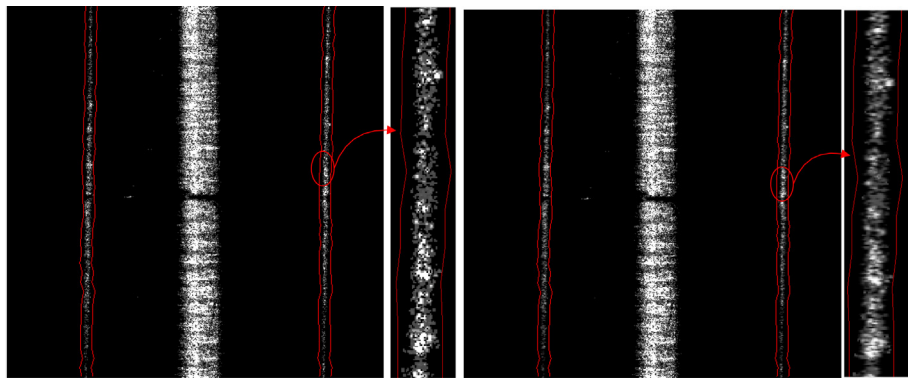


**Fig. 12.** The images of  $ROI_r$  before and after median filter process.

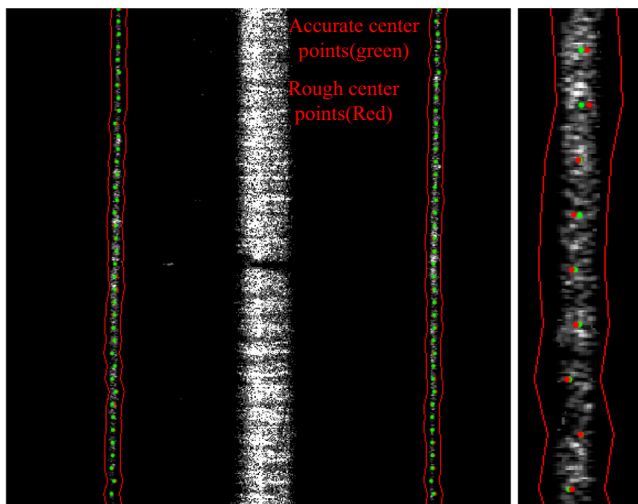


**Fig. 13.** The accurate center point located by gray level weighting method.

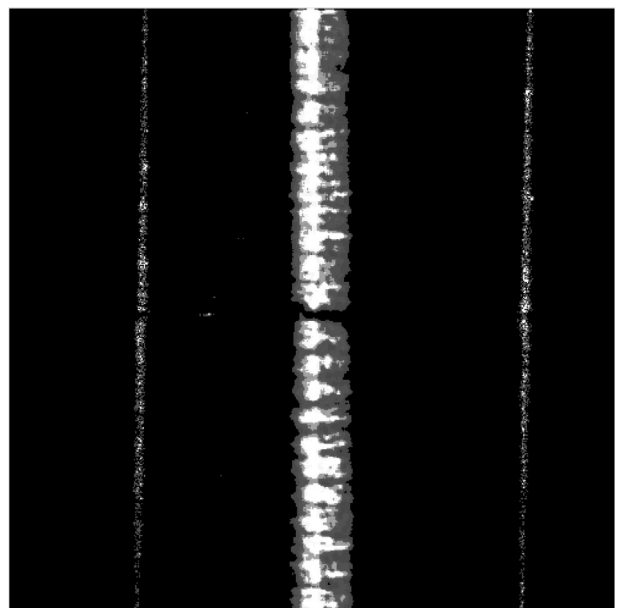


**Fig. 15.** Median filter process.

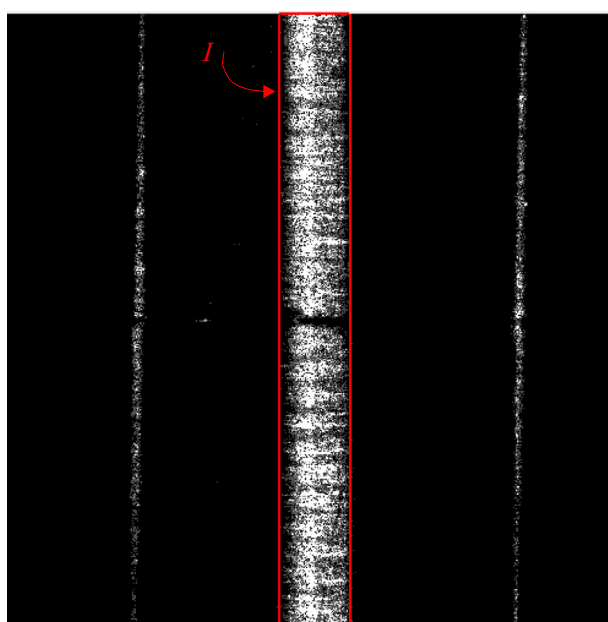


**Fig. 14.** The green laser stripe area  $I$ .

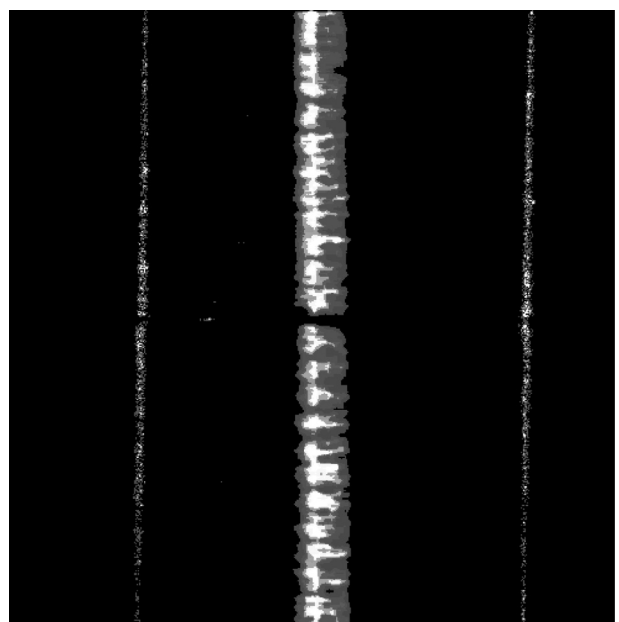


**Fig. 16.** Morphological closing process.

$$\varepsilon_B(I_f)(i,j) = \min_{(k,l) \in B_{(i,j)}} I_f(k,l) \quad (4)$$

Similarly, the dilation  $\delta_B(I_f)$  is given as

$$\delta_B(I_f)(i,j) = \max_{(k,l) \in B_{(i,j)}} I_f(k,l) \quad (5)$$

Thus, morphological opening is given by  $\gamma_B(I_f) = \delta_B(\varepsilon_B(I_f))$ . Let  $I_{fm}$  denote the image after morphological opening process.

Thirdly, as shown in Fig. 17, the rough center point of the weld seam is located and region of interest is extracted. Since the gray value of the weld seam is much lower than that of the weld face, the approximate position of weld seam can be located by gray-level integration projection. The corresponding equation is given as

$$S(i) = \sum_{j=500-50}^{500+50} \frac{1}{3} [I_{fm}(i-1,j) + I_{fm}(i+1,j) + I_{fm}(i,j)], 1 \leq i \leq 1000 \quad (6)$$

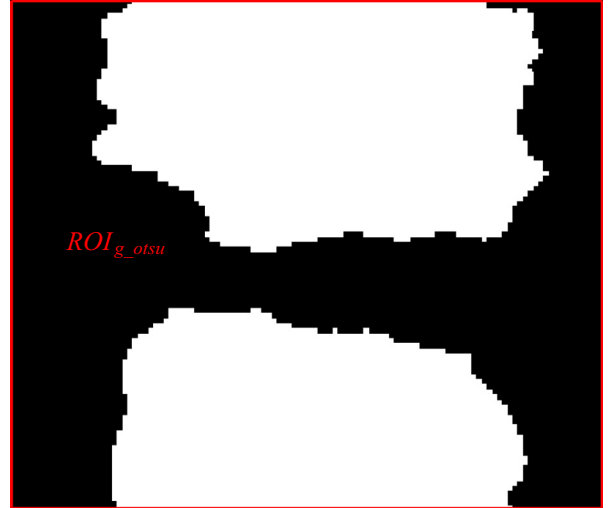


Fig. 19. OTSU threshold process.

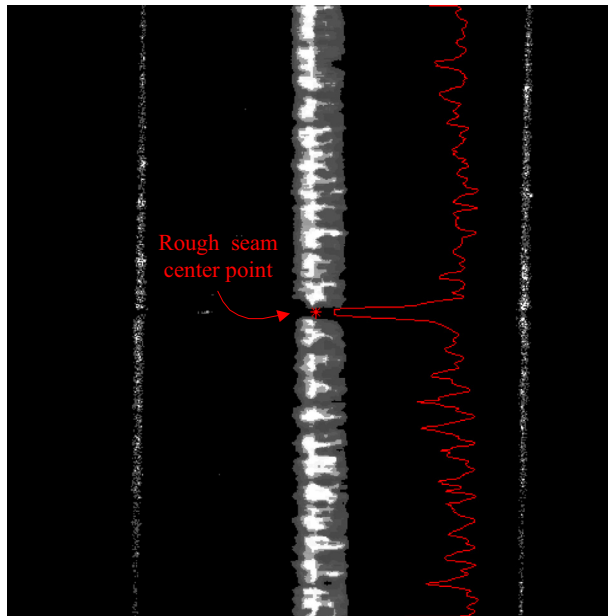


Fig. 17. Gray-level integration projection process.

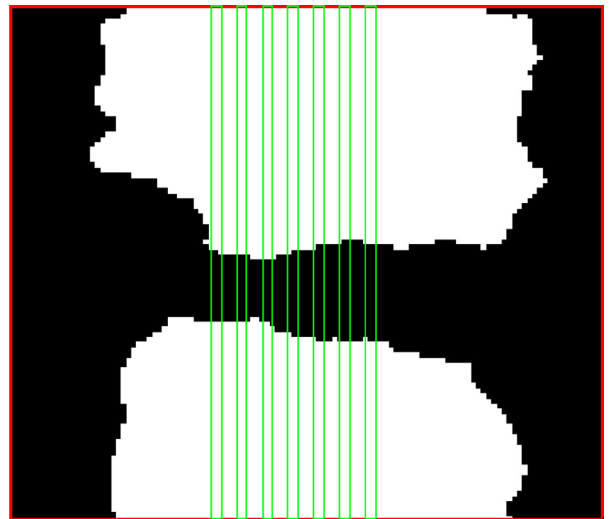


Fig. 20. Vertically sampling.

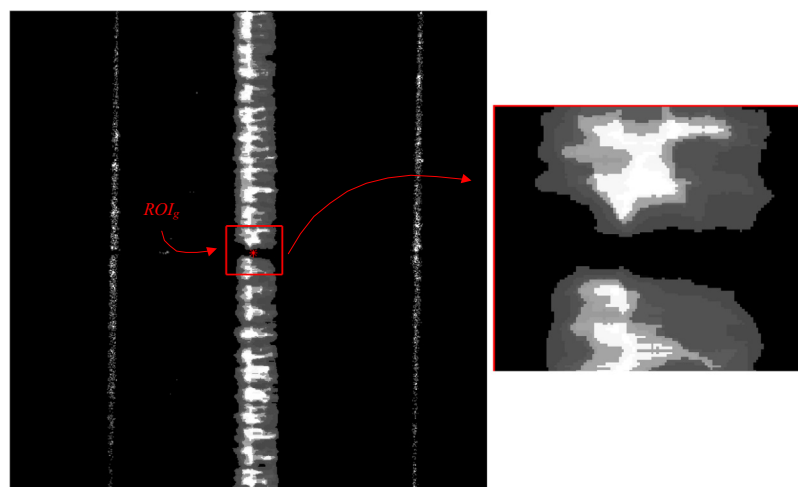


Fig. 18. The region of interest  $ROI_g$ .

where  $S(i)$  is the average gray value of all the pixels in row  $i - 1, i$  and  $i + 1$ . As shown in Fig. 17,  $S(i)$  gets its smallest value in row  $R_{\min}$ . Thus, the point  $(R_{\min}, 500)$  in image coordinate can be regarded as the rough position of the weld seam. As the width of the weld seam is less than 0.3 mm and its centerline is approximately perpendicular to the vertical centerline of the image, the region of interest  $ROI_g = \{(i, j) | R_{\min} - 50 \leq i \leq R_{\min} + 50; 450 \leq j \leq 550\}$  with 100 rows can be extracted, which is shown in Fig. 18.

Next, as shown in Fig. 19, OTSU threshold method based on adaptive thresholding is used to determine the threshold in  $ROI_g$ , which helps to separate the weld seam from the background. The edge of the weld seam is very distinctive in the processed image  $ROI_{g\_otsu}$ .

To speed up the image process, as shown in Fig. 20, vertically sampling is adopted to get seven banded image regions from  $ROI_{g\_otsu}$ . Every banded image region has the width of 3 pixels. These seven banded sub-images are extracted by two steps. Firstly,  $l_1 : (u - 15) = 0 l_2 : (u - 10) = 0, \dots, l_7 : (u + 15) = 0$  are obtained by moving the centerline  $l : u = 0$  parallel to the left and the right side by 5 pixels respectively. Secondly, when each of seven three lines is taken as centerline of a banded area, seven banded sub-images with a width of 3 pixels each can be extracted conse-

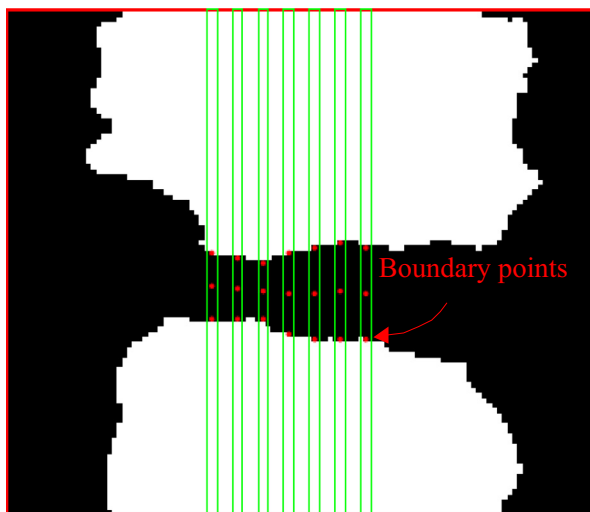


Fig. 21. Boundary points of weld seam.

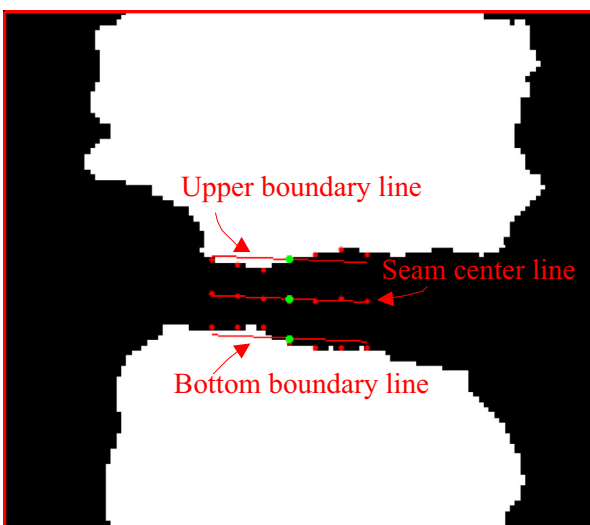


Fig. 22. Seam center and center line.

quently. A search window with 3 pixels width and 5 pixels height is used to locate the seam edge in each sub-image. When the average value of grey value in the search window reaches threshold, the center point in search window is regarded as the edge point of the weld seam. When the threshold is 100, the boundary points can be extracted exactly. In this manner, as shown in Fig. 21, the boundary points of weld seam in the seven banded images can be obtained.  $T_l(S_{xn}^T, S_{yn}^T), (n = 1, 2, \dots, 7)$  are the upper boundary points.  $B_l(S_{xn}^B, S_{yn}^B), (n = 1, 2, \dots, 7)$  are the bottom boundary points. Similarly,  $C_c(S_{xn}^C, S_{yn}^C), (n = 1, 2, \dots, 7)$  are center points, which are obtained by computing the average values of the corresponding boundary points. Thus, the center line of the weld seam can be obtained through least square fitting method. The center point of the seam center line is regarded as seam center point. The seam center and center line are shown Fig. 22.

Let  $K_s$  denote the slope of seam center line  $l_c$ . The slope of upper boundary line  $l_u$  and bottom boundary line  $l_b$  is assumed to be equal to that of line  $l_c$ . In addition, the average values of the boundary points in upper boundary and bottom boundary are given as follows:

$$\begin{cases} S_{Gx}^T = \left( \sum_{n=1}^7 S_{xn}^T \right) / 7 \\ S_{Gy}^T = \left( \sum_{n=1}^7 S_{yn}^T \right) / 7 \end{cases} \quad (7)$$

$$\begin{cases} S_{Gx}^B = \left( \sum_{n=1}^7 S_{xn}^B \right) / 7 \\ S_{Gy}^B = \left( \sum_{n=1}^7 S_{yn}^B \right) / 7 \end{cases} \quad (8)$$

Table 2  
The configuration of weldment.

Parameters	Description
Welding type	Laser welding
Type of joint	Butt joint
Plate thickness	1.5 mm
Seam width	0.05–0.1 mm
Seam length	1500 mm



Fig. 23. The simulative weldment.

**Table 3**

The measurement comparison.

Seam width measured by TESA-VISIO (mm)	Seam width measured by the proposed sensor (mm)	
	Mean	Average deviation
0.04	0.045	0.005
0.05	0.054	0.004
0.06	0.062	0.002
0.07	0.075	0.005
0.08	0.076	-0.004
0.09	0.092	0.002
0.10	0.101	0.001

Thus, the equation of the boundary line  $l_T$  and  $l_B$  in image coordinate OUV is computed as follows:

$$v = K_s(u - S_{Gx}^T) + S_{Gy}^T \quad (9)$$

$$v = K_s(u - S_{Gx}^B) + S_{Gy}^B \quad (10)$$

The distance between the two parallel lines  $l_T$  and  $l_B$ , is the width of weld seam. Let it denote  $W_s$  in pixel unit, which has the following expression:

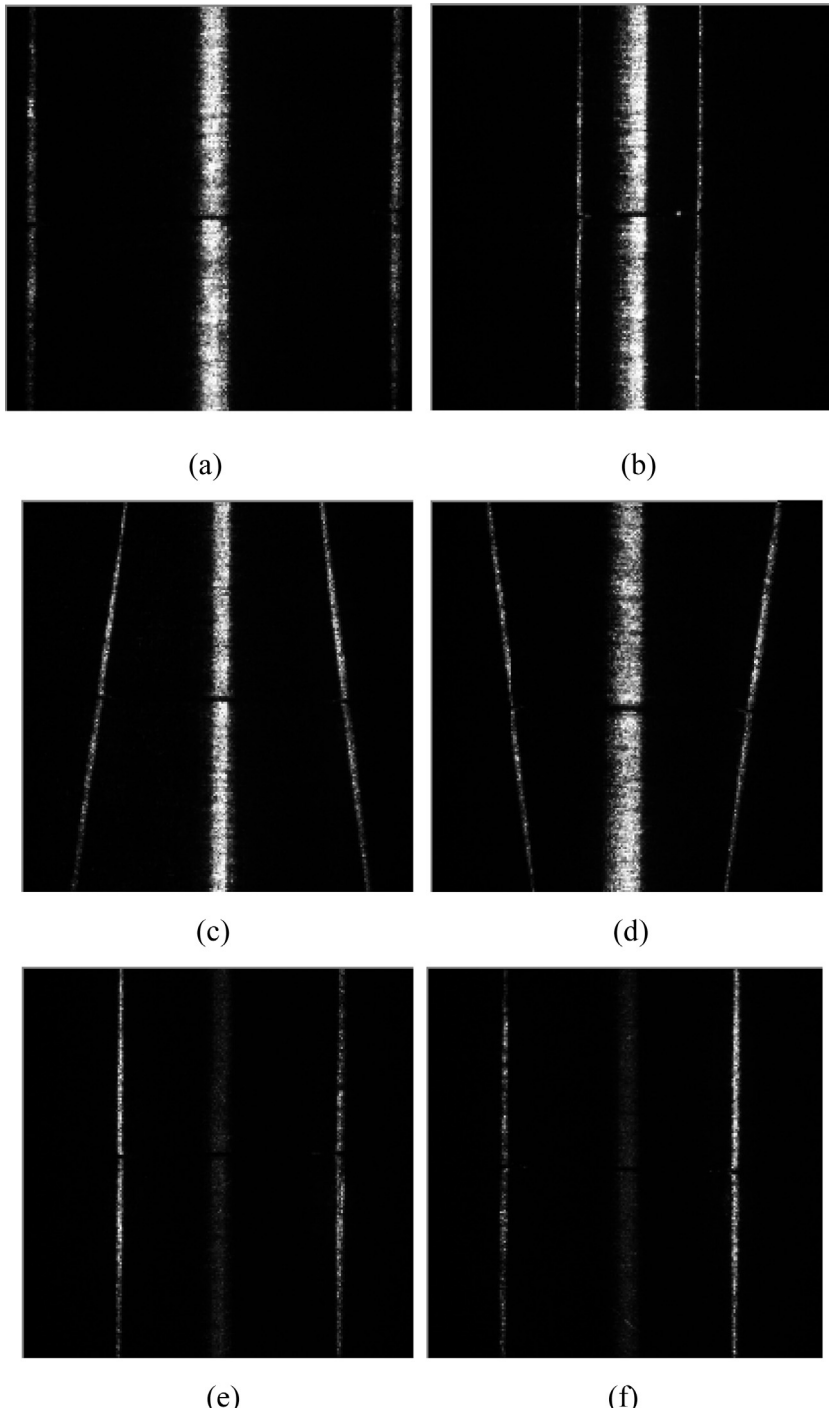


**Fig. 24.** Weld seam images captured under different measurement position.

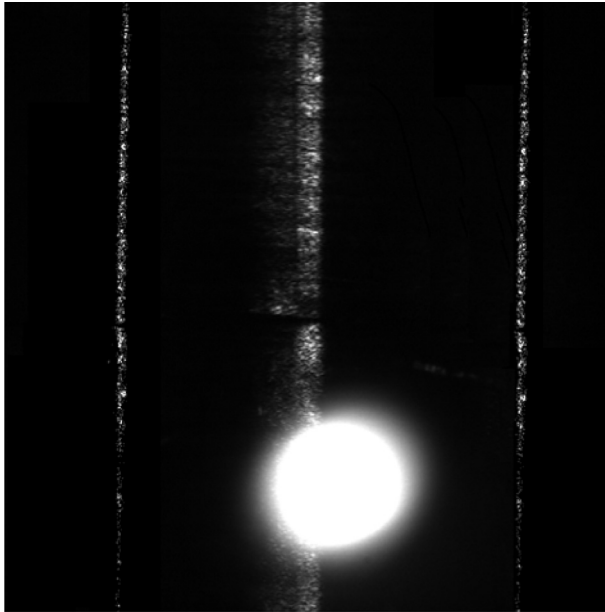


**Fig. 25.** Weld seam images with spark.

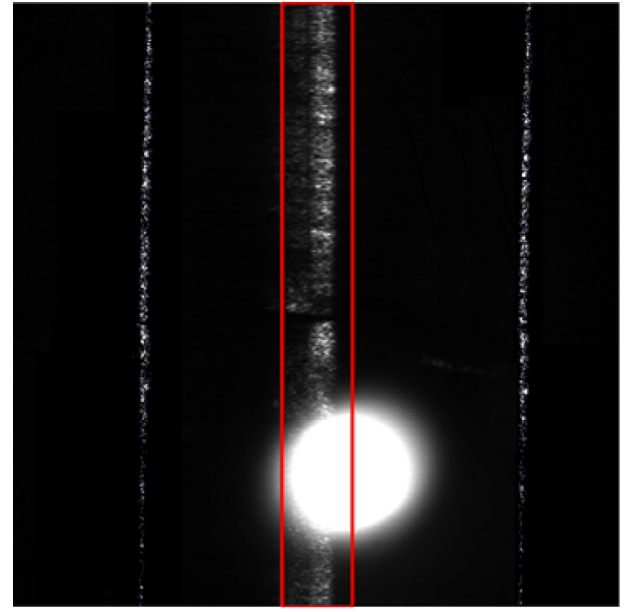


**Fig. 27.** The green laser stripe area.

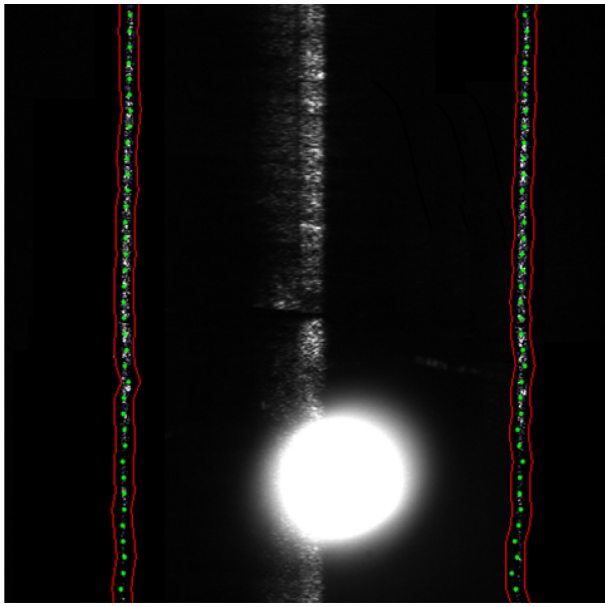


**Fig. 26.** Center point extraction of the red laser stripes.

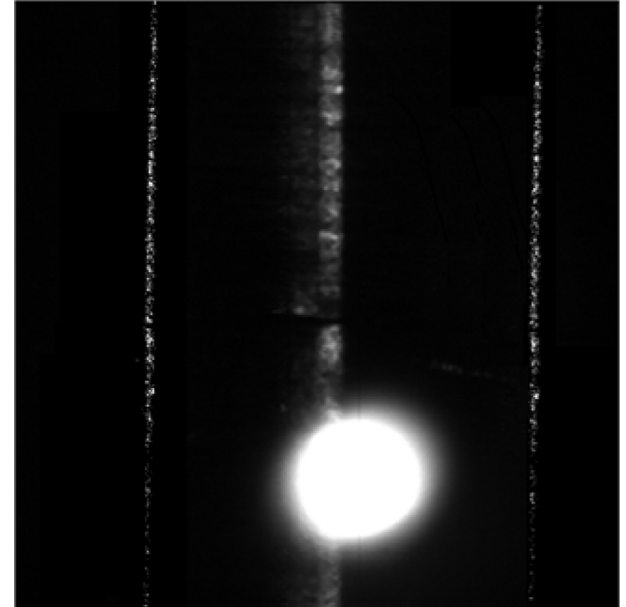


**Fig. 28.** Median filter.

$$W_s = \frac{\left| (S_{Gy}^T - S_{Gy}^B) - K_s (S_{Gx}^T - S_{Gx}^B) \right|}{\sqrt{1 + K_s^2}} \quad (11)$$

#### 4. Experiment results

To confirm the vision sensor and its corresponding algorithm's effectiveness, the vision sensor was mounted on a multi-axis Computer Numerical Control (CNC) welding machine for laser welding. The configuration of the weldment and the welding system are listed in Table 2, under which the measurements are carried out.

Firstly, to demonstrate the measurement precision of seam width, experiments were carried out to a simulative weldment whose seam width can be adjusted manually. The measurement

results of the weld seam center and width are compared with that of a commercial image measuring apparatus (TESA-VISIO 300). Numerous weld seam images were captured and processed. The simulative weldment and the comparison are shown in Fig. 23 and Table 3, respectively. The average deviation is less than 0.005 mm. The results of the experiment reveals that weld seam with width (0.04–0.1 mm) can be measured accurately. As the weld seam center is computed by the seam boundary points, its precision is regarded as same as that of the weld seam width.

Secondly, to verify the measurement precision of the normal vector of the weld face and the distance between the laser focus and the fitting plane, the vision sensor is adjusted to certain different positions by moving the corresponding axis of the CNC welding machine to measure the same weld face. Three types of measurements are designed. Firstly, as shown in Fig. 24(a) and (b), the

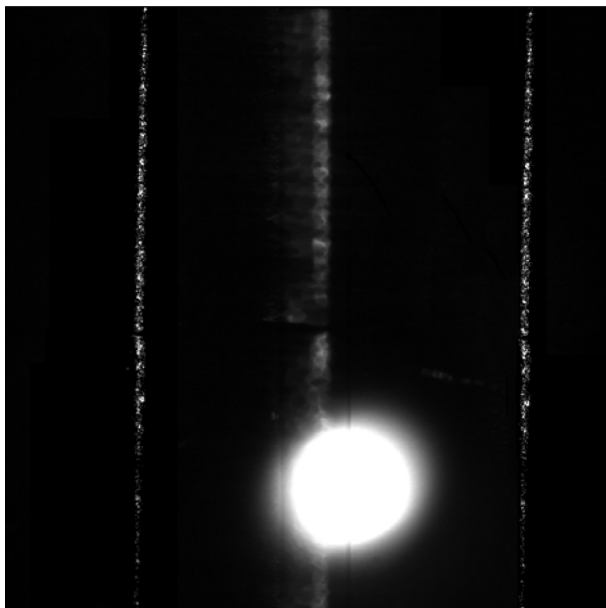


**Fig. 29.** Morphological closing process.



**Fig. 31.** OTSU threshold process.

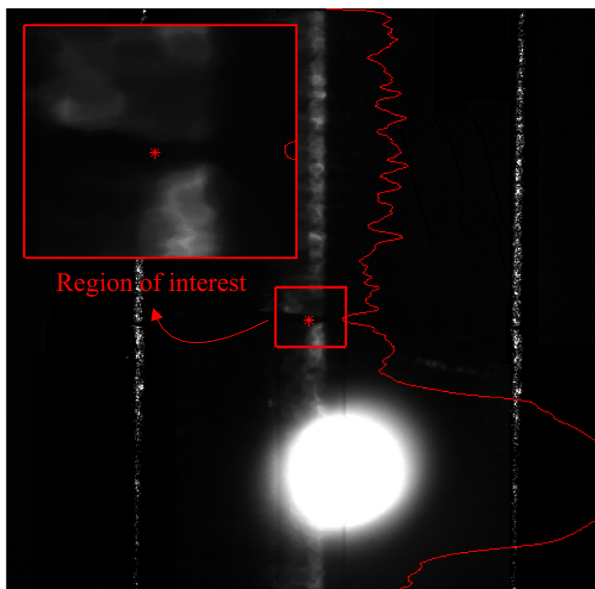


**Fig. 30.** ROI located by Gray-level integration projection.

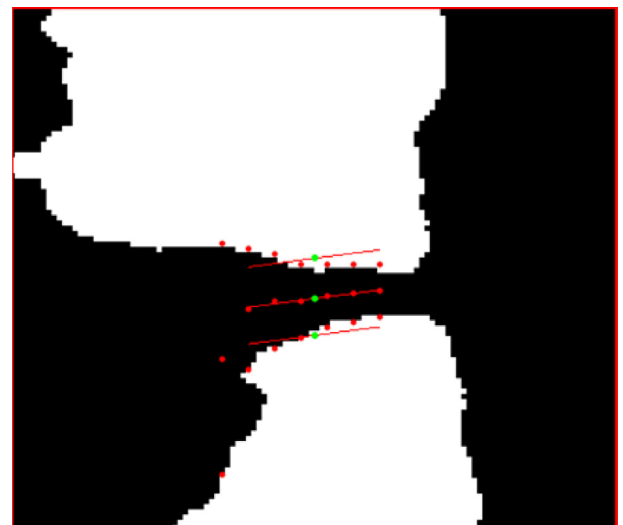


**Fig. 32.** Seam center and center line.

optical axis of the vision sensor is vertical to the weld face while the position of vision sensor is different in the Z axis. Secondly, as shown in Fig. 24(c) and (d), the optical axis of the vision sensor is rotated  $+10^\circ$  and  $-10^\circ$  along X axis, respectively, while the weld face is vertical to the Z axis. Thirdly, as shown in Fig. 24(e) and (f), the optical axis of the vision sensor is rotated  $+5^\circ$  and  $-5^\circ$  along Y axis, respectively, while the weld face is vertical to the Z axis. It is demonstrated through numerous experiments of this type that the average measurement error of normal vector is less than  $3^\circ$ , and the average measurement error of the distance between the laser focus and the fitting plane is less than 0.12 mm.

Thirdly, as there are sparks and fumes during laser welding process, weld seam images with heavy light noise are particularly analyzed. Owing to the image principle of telocentric lens, only highly collimated rays are admitted. As a result, as shown in Fig. 25, weld seam feature is still very distinctive, although there are sparks

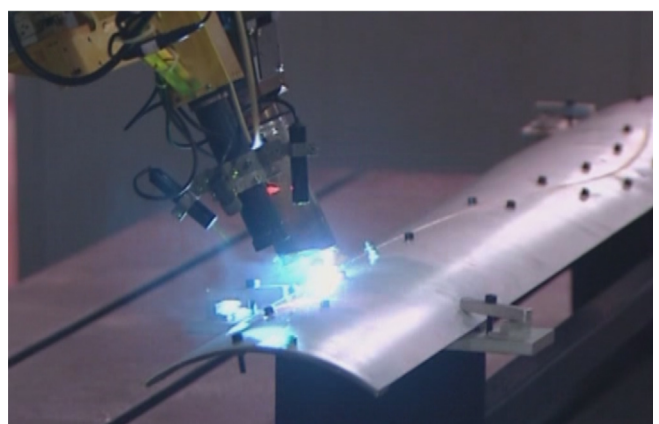


**Fig. 33.** Laser welding experiment.

captured by the vision sensor. As shown in Fig. 26, the center points of the red laser stripes are extracted exactly by the proposed algorithm even under this situation. As the spark covers part of the green laser stripe, the detailed images processed by (Figs. 27–32) are given to verify the robustness of the proposed algorithm. After the median process in Fig. 28 and morphological closing process in Fig. 29, the rough center position of the weld seam is located correctly by gray-level integration projection in Fig. 30 despite the influence of the spark. As the ROI shown in Fig. 31, the OTSU threshold method effectively separates the weld seam from the background. Finally, the weld seam center point, the weld seam center line and boundary lines are extracted precisely (see Fig. 32).

In addition, thanks to the design of the vision sensor, only part of the weld seam image has to be processed. Moreover, fast searching method is adopted, ROI areas are extracted and sampling analysis method is employed, so that the every image can be processed within 10 ms. As welding experiment shown in Fig. 33, the welding torch can follow the weld seam trajectory at a welding speed of 5 m·min<sup>-1</sup>.

## 5. The conclusion

A weld seam vision sensor and its corresponding image process algorithm for the detection of narrow butt joint weld seam with width less than 0.1 mm are proposed in this article. The vision sensor, which uses three laser stripes for different measurement purpose, combines the two-dimensional measurement method and the three-dimensional measurement method. Seam width, seam center position and the normal vector can be measured simultaneously in a single weld seam image. The proposed image process algorithm is very effective even under heavy light noise caused by laser welding and can meet the real-time requirements of high speed laser welding. Experiment shows that the average measurement error of the weld seam width and the weld seam center is less than 0.005 mm, the average measurement error of normal vector of the weld face is less than 3° and the average measurement

error of the distance between the laser focus and the fitting plane is less than 0.12 mm.

## References

- [1] H.B. Ma, S. Wei, Zh.X. Sheng, Robot welding seam tracking method based on passive vision for thin plate closed-gap butt welding, *Int. J. Adv. Manuf. Technol.* 48 (9–12) (2010) 945–953.
- [2] J.W. Kim, J.H. Shin, A study of a dual-electromagnetic sensor system for weld seam tracking of I-butt joints, *Proc. Inst. Mech. Eng. B, J. ENG. Manuf.* 217 (9) (2003) 1305–1313.
- [3] S.B. Chen, X.Z. Chen, T. Qiu, Acquisition of weld seam dimensional position information for arc welding robot based on vision computing, *J. Intell. Robot. Syst.* 43 (1) (2005) 77–97.
- [4] H.Y. Shen, H.B. Ma, T. Lin, Research on weld pool control of welding robot with computer vision, *Industrial. Robot. Int. J.* 34 (6) (2007) 467–475.
- [5] D.Y. You, X.D. Gao, S. Katayama, Review of laser welding monitoring, *Sci. Technol. Weld. Join.* 9 (3) (2014) 181–201.
- [6] T. Qin, K. Zhang, J. Deng, et al., Image processing methods for V-shape weld seam based on laser structured light, *Found. Intell. Syst.* 122 (2011) 527–536.
- [7] Q.Q. Wu, J.P. Lee, M.H. Park, et al., A study on the modified Hough algorithm for image processing in weld seam tracking, *J. Mech. Sci. Technol.* 29 (11) (2015) 4859–4865.
- [8] Y. He, H. Chen, Y. Huang, et al., Parameter self-optimizing clustering for autonomous extraction of the weld seam based on orientation saliency in robotic MAG welding, *J. Intell. Rob. Syst.* 83 (2) (2016) 219–237.
- [9] P. Kiddee, Z. Fang, M. Tan, An automated weld seam tracking system for thick plate using cross mark structured light, *Int. J. Adv. Manuf. Technol.* 87 (9–12) (2016) 1–15.
- [10] Y. Huang, G. Li, W.J. Shao, et al., A novel dual-channel weld seam tracking system for aircraft T-joint welds, *Int. J. Adv. Manuf. Technol.* (2016) 1–11.
- [11] L. Zhang, W. Ke, Q. Ye, et al., A novel laser vision sensor for weld line detection on wall-climbing robot, *Opt. Laser Technol.* 60 (2) (2014) 69–79.
- [12] Y. Xu, G. Fang, S. Chen, Real-time image processing for vision-based weld seam tracking in robotic GMAW, *Int. J. Adv. Manuf. Technol.* 73 (9) (2014) 1413–1425.
- [13] Z. Fang, D. Xu, M. Tan, Visual seam tracking system for butt weld of thin plate, *Int. J. Adv. Manuf. Technol.* 49 (5) (2010) 519–526.
- [14] H. Chen, K. Liu, G. Xing, A robust visual servo control system for narrow seam double head welding robot, *Int. J. Adv. Manuf. Technol.* 71 (9) (2014) 1849–1860.
- [15] X. Gao, Detection of micro gap weld using magneto-optical imaging during laser welding, *Int. J. Adv. Manuf. Technol.* 73 (1) (2014) 23–33.
- [16] P.J. Wang, W.J. Shao, S.H. Gong, et al., High-precision measurement of weld seam based on narrow depth of field lens in laser welding, *Sci. Technol. Weld. Joining* 21 (4) (2016) 267–274.